

# Observations on the fracture and deformation behaviour during annealing of residually stressed polycrystalline aluminium oxides

Y. TREE, A. VENKATESWARAN, D. P. H. HASSELMAN

*Department of Materials Engineering, Virginia Polytechnic Institute and State University, Blacksburg, Virginia 24061, USA*

Highly residually stressed polycrystalline aluminium oxides were found to exhibit residual stress relaxation, as evidenced by changes in load-bearing ability, at temperatures as low as about 850° C. This temperature is much too low for such relaxation to occur by dislocation, Nabarro–Herring or Coble creep. Irreversible changes in specimen dimension coupled with SEM-fractography revealed that the stress relaxation resulted from creep by intergranular cavitation and crack propagation. In one aluminium oxide, such cavitation and crack propagation appeared to take place in a stable mode along a viscous glassy grain boundary phase. In high-purity fine-grained aluminium oxide, crack propagation occurred in a frequently totally catastrophic and highly unstable manner. This latter material was also observed to exhibit spontaneous fatigue during isothermal anneal. Implications of the findings of this study for the use of thermal anneals to promote residual stress relaxation in structural ceramic materials are discussed.

## 1. Introduction

Residual stresses can have a profound effect on the properties and performance of engineering ceramics. Such stresses can arise from many sources including non-isothermal conditions or variable furnace atmosphere encountered during sintering, thermoviscoelastic effects, spatially nonuniform thermal expansion, phase transformations, or other phenomena [1–6].

Residual stresses introduced under controlled conditions can be used for purposes of property enhancement, such as the strengthening of glass by tempering or ion-exchange [7, 8].

Usually, however, residual stresses are highly undesirable. A number of non-destructive methods for the measurement of residual stresses based on photoelastic, X-ray, ultrasonic, spectroscopic and other principles are available [9–12]. Nevertheless, the complete mapping of the magnitude and distribution of a three-dimensional residual stress field, if practical at all, still is subject to considerable error. For this reason, the existence of residual stresses of unknown magnitude in components or

structures can introduce large uncertainty in their design and engineering performance. A further complexity is introduced by the usual multi-axial nature of residual stress distributions for which failure predictions are less well established compared to a uniaxial stress state.

Residual stress relaxation during an isothermal anneal or during actual use of a component can lead to geometric distortions, which can have an adverse effect on the performance of components made to high dimensional precision.

In extreme cases, residually stressed brittle materials such as polycrystalline silicon [13] vapour-deposited silicon carbide [14], tempered glass [15] and large ceramic structures [16] exhibit a time-dependent spontaneous and frequently explosive fracture at room temperature, presumably as the result of sub-critical crack growth due to humidity-enhanced stress corrosion.

As an alternative to their measurement, residual stresses may be reduced or even eliminated by appropriate treatments such as the commonly used isothermal anneal. In ductile metallic materials,

residual stress relaxation is expected to occur readily by dislocation-controlled creep at low or moderate homologous temperatures. In brittle ceramic materials, the temperatures of an anneal should be sufficiently high that stress relaxation can occur by diffusional processes such as Nabarro–Herring [17, 18] or Coble [19] creep. The resulting rate of stress relaxation is expected to be affected by the presence of a viscous grain boundary phase. The nature of the multi-axial residual stress state, which may enhance or suppress deformation by shear also is expected to play a significant role.

Only a few quantitative studies of the mechanisms and kinetics of the residual stress relaxation in structural ceramics appear to have been carried out. One such study by Cockbain [1] showed that an isothermal anneal was unsuccessful in removing residual stresses in hot-pressed silicon nitride. The study of Krohn *et al.* [20] showed the relaxation of residual stresses in a coarse-grained (about 25  $\mu\text{m}$ ) polycrystalline aluminium oxide to occur at temperatures as low as 850° C. In view of the mechanisms of creep known at that time, these observations were interpreted to represent evidence for the existence of Coble creep. It should be noted, however, that the calculated rate of Coble creep at 850° C is too low to explain the observed stress relaxation.

Crack growth, as discussed earlier, can play a significant role in the mechanical behaviour of residually stressed brittle materials as evidenced by their spontaneous failure. It is also known [21], that due to the accompanying decrease in elastic moduli, the growth of cracks leads to a time-dependent increase in elastic strain, referred to as elastic creep by crack growth. As shown by Weertman [22] the presence of cracks can lead to an acceleration of the rate of deformation of a creep mechanism operative in the absence of cracks. In polycrystalline ceramics, such cracks exist in the form of intergranular pores at grain boundaries or triple points.

In brittle materials, crack growth can occur at levels of temperature well below those at which significant creep deformation can take place. For this reason, at modest or low homologous temperatures, creep by crack growth may well constitute the only mechanism by which residual stress relaxation in brittle materials can occur. For this reason, it is postulated that the observations of Krohn *et al.* [20] of the residual stress

relaxation in polycrystalline alumina at 850° C could be due to the presence and growth of cracks. Such a mode of stress relaxation would be highly undesirable, as crack formation could lead to a significant weakening.

In this respect, then, the purpose of the present study, was to conduct an experimental programme on the effect of a thermal anneal on residually stressed brittle ceramics, with special emphasis on the possible role of crack formation.

## 2. Experimental details

### 2.1. Materials

Three polycrystalline aluminium oxides in the form of circular rods, were obtained from commercial sources as listed in Tables IA and IB together with their mean grain size, diameter and principal impurities as identified by microprobe analysis. The magnesium in the 614 and 838-aluminas probably occurs in the form of MgO added as a grain growth inhibitor. The Al-300 alumina was nominally identical to the one studied by Krohn *et al.* [20]. Scanning electron micrography (SEM) of specimens broken at room temperature showed transgranular fracture, typical for these materials. The Al-300 alumina exhibited pore sizes as large as a few microns. Most of these pores occurred at triple points or grain boundaries. Pore sizes in the 614 and 838 alumina were of the order of fractions of a  $\mu\text{m}$ .

Fig. 1 shows the distribution of the silicon in the Al-300 alumina. The calcium and iron were found to occur in the same position as the silicon. The location of these impurities suggest that they exist in the form of an iron–calcium–aluminium–silicate glass at the grain boundaries.

Fig. 2 shows the distribution of the silicon in the 614 alumina, which coincided with the location of the calcium and magnesium. Comparison with Fig. 1 indicates that the 614-alumina has a smaller amount of glassy phase at the grain boundary than the Al-300 alumina. Microprobe analysis of the 838-alumina showed only very faint evidence of the impurities, suggestive of the near or complete absence of a glassy grain boundary phase.

### 2.2. Residual stressing and annealing treatment

Following the general methods of Kirchner [3], the alumina rods, cut to a length of about 3.75 cm, were residually stressed by a tempering treatment which consists of quenching from an

TABLE IA Alumina materials selection

Material	Commercial source	Mean grain size ( $\mu\text{m}$ )	Diameter of rod (mm)
Al-300	Western Gold and Platinum Co., Belmont, CA	25	5.04
ALSIMAG 614	American Lava Corp., 3M Company, Chattanooga, TN	5	4.81
ALSIMAG 838	American Lava Corp., 3M Company, Chattanooga, TN	4	4.83

TABLE IB Grain and grain-boundary composition\* of the aluminas

(element)	Al-300		ALSIMAG 614		ALSIMAG 838	
	Grain	Grain boundary	Grain	Grain boundary	Grain	Grain boundary
Al as $\text{Al}_2\text{O}_3$	99.79	32.26	99.77	77.66	99.76	92.69
Ca as CaO	0.00	27.61	0.01	0.97	0.00	1.34
Si as $\text{SiO}_2$	0.00	37.52	0.09	18.94	0.00	1.48
Mg as MgO	0.04	0.69	0.05	1.08	0.04	3.37
Fe as FeO	0.03	0.80	0.03	0.07	0.02	0.07

\*All data are given in wt %.

inductively heated graphite susceptor into silicone oil\* at room temperature. For the Al-300 and 614 alumina, the susceptor temperature was 1450 and 1550°C, respectively. For the 838 alumina two susceptor temperatures of 1550 and 1600°C were used. The residual stresses result from thermo-viscoelastic stress relaxation during quenching. Upon return to thermal equilibrium, the residual stress state is compressive in the surface regions and tensile in the interior regions of the specimens. The existence of such an internal stress contribution can be demonstrated by the slotted-rod test [3] or by a measurement of the tensile strength by means of a bend test, in which the tensile stresses in the outer fibre of the specimen must first overcome the compressive stresses in the surface, before failure can occur. The rods were held in the heated susceptor for approximately 10 min to assure thermal equilibrium prior to the quench. As judged by a strength test (in bending), annealing treatment of the as-received rods prior to the tempering process appeared to have no effect on the magnitude of the residual stress, presumably because of the subsequent anneal in the heated graphite susceptor. No attempts were made to measure the magnitude of the residual stresses by non-destructive means. Nevertheless, a feasibility

study of the applicability to measure such stresses by the spectroscopic method described by Grabner [12] is intended to be the subject of a future report.

All thermal annealing treatments were carried out in a dilatometer<sup>†</sup>. This permitted close control of the specimen temperature as well as the monitoring of dimensional changes due to the formation of cracks and the range of temperature over which these occurred. In order to meet the dimensional requirements of the dilatometer all specimens were cut to a length of about 2.2 cm. Three different thermal annealing schedules were followed. The first schedule consisted of heating and cooling at a rate of 10°C min<sup>-1</sup> to 1000°C, with special emphasis on monitoring dimensional changes. The second annealing schedule consisted of heating at 10°C min<sup>-1</sup> to a prescribed temperature followed by holding for 25 min and cooling to room temperature. The residually stressed specimens were subjected to a strength test for the purpose of ascertaining any structural damage which may have resulted from the formation of cracks. The third annealing treatment used primarily for the 838 alumina, consisted of heating the specimen at 5°C min<sup>-1</sup> to a prescribed temperature, followed by holding for a period up to

\*Dow Corning, Type 200, 100 Cst.

<sup>†</sup>Dupont, Thermo-Mechanical Analyzer Model No. 943.

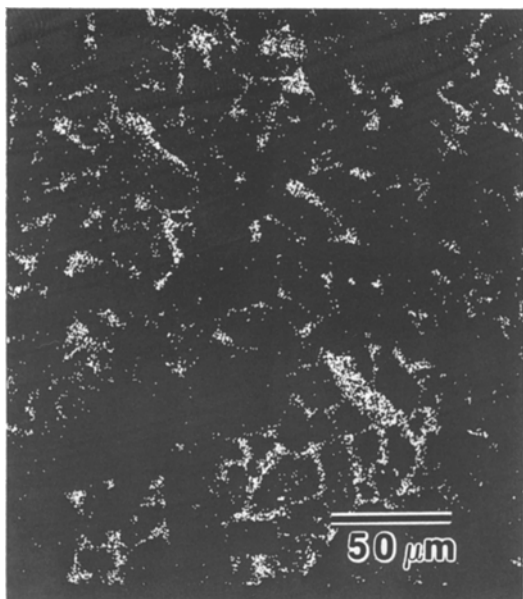


Figure 1 Distribution of silicon in Al-300 alumina.

24 h. This annealing schedule permitted observation of the spontaneous fracture due to fatigue under the influence of the residual stresses. For this latter purpose, the dilatometer was modified to include a clock which recorded the instant of failure, when triggered by the signal from the dilatometer due to the discontinuous change in length on fracture.

Any structural damage in the specimen due to crack formation was measured in a bend test at

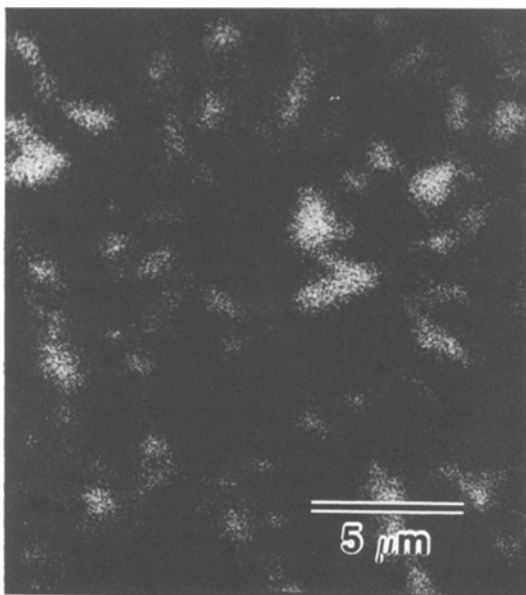


Figure 2 Distribution of silicon in 614 alumina.

room temperature. The tensile fracture stress was calculated from the load at fracture assuming that the specimen was homogeneous, i.e. the elastic properties were uniform over the total cross-sectional area. Due to the small size of the specimens, this test was limited to 3-point bending using centre-point loading with a total span of 1.27 cm. This resulted in a rather high diameter to span ratio and values of strength higher than would have been obtained in 4-point bending or with a lower diameter to span ratio. For this reason, more attention should be paid to the comparative behaviour rather than the absolute values of strength.

Scanning electron fractography was used to ascertain the mode of crack formation and propagation.

### 3. Experimental observations

#### 3.1. Al-300 Alumina

Figs. 3a and b compare the thermal expansion behaviour of an as-received annealed and a tempered specimen of the Al-300 alumina, respectively. For the as-received specimen the data agree very well with the recommended behaviour for a dense high-quality polycrystalline alumina [23]. In contrast, the tempered specimen shows a smooth monotonic irreversible increase in length during the heating portion of the cycle over the temperature range from about 850 to 900°C. Since this alumina is in the stable  $\alpha$ -form, this irreversible increase in length cannot be attributed to a crystallographic phase transformation. Most likely, the permanent increase in length can be attributed to internal cavitation and/or the formation of cracks.

Fig. 4 shows the tensile strength measured in bending, following the 25 min anneal over a range of annealing temperatures. Included in Fig. 4 are the values of strength at room temperature of the as-received and tempered specimens. These latter data represent the mean and range of individual data for sets of 10 specimens. The strength for the annealed specimen represents the average of 4 specimens. It is evident that the tempering causes a significant increase in strength. At the higher values of annealing temperature, the strength is reduced to near that of the as-received material, in agreement with the earlier observations of Krohn *et al.* [20]. Since the irreversible change in length and the strength loss occurs over the same temperature range, it is expected that both these effects are caused by the same phenomenon.

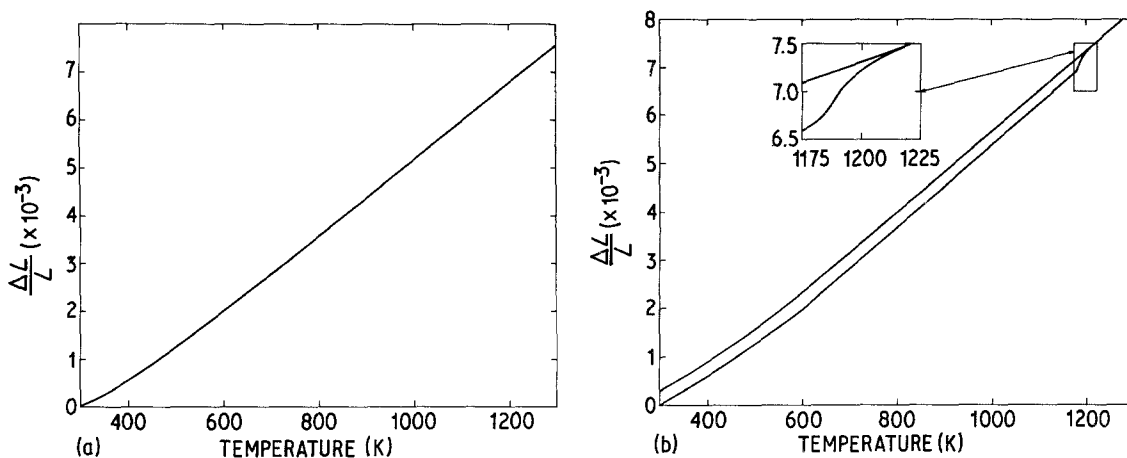


Figure 3 Thermal expansion of (a) as-received and annealed and (b) tempered Al-300 alumina.

Fig. 5 presents evidence which confirms the earlier hypothesis that the irreversible increase in length of the tempered specimen shown in Fig. 3b is due to cavitation and/or crack growth. Fig. 5a is a scanning electron fractograph of a tempered and annealed specimen broken at room temperature, in the region within the specimen originally subjected to a compressive residual stress. This fracture surface in view of the existence of cleavage patterns on some of the grains indicates that crack propagation occurred at room temperature during the strength test. In contrast, Fig. 5b shows a fracture surface in the central regions of the specimen originally subjected to a tensile residual stress state. This fracture which is exclusively intergranular,

is typical of fracture at an elevated temperature. Fig. 5b also clearly shows the existence of a glassy grain boundary phase, as well as grain boundary separation perpendicular to the fracture surface, presumably due to the existence of radial and/or tangential tensile stresses. The most likely explanation for the differences in fracture behaviour shown in Figs. 5a and b, is that the crack propagation at room temperature followed the plane of the cracks formed at the high temperature.

It is suggested that the grain boundary separation in the Al-300 occurred at temperatures at which the viscosity of the glassy-grain boundary phase becomes sufficiently low that, during the time of

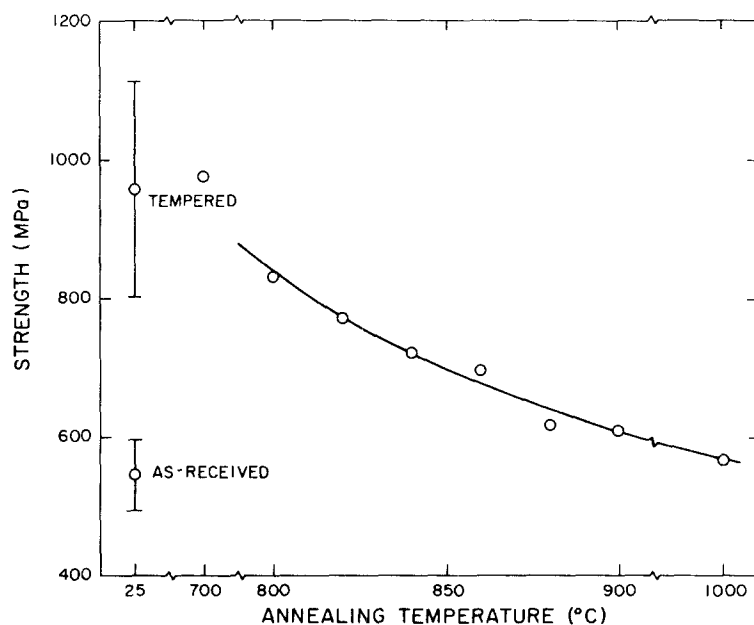
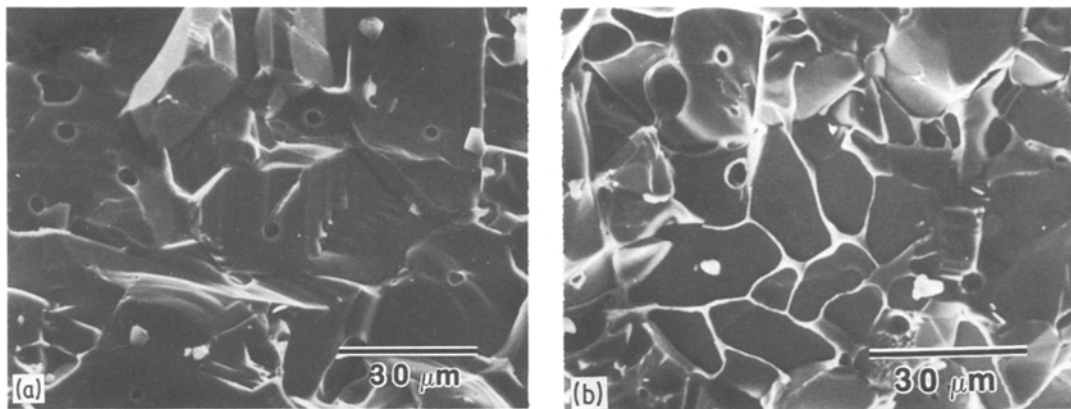


Figure 4 Tensile strength at room temperature as measured in bending of tempered Al-300 alumina after 25 min anneal, as a function of annealing temperature.



**Figure 5** SEM fractographs of tempered Al-300 alumina specimen broken at room temperature, following an anneal at 900° C for 25 min. (a) Surface region originally under compressive residual stress. (b) Central region of specimen originally subjected to tensile residual stress.

anneal, the glass could deform significantly by viscous flow. Such viscous flow is clearly evident in the SEM fractograph shown in Fig. 6. The same phenomenon is indicated in Fig. 7 which shows a remnant of the grain boundary phase typical of the “finger-like” growth described by Fields and Ashby [24]. This suggests that cracks grew from one side of the grain boundary facet to the other, possibly having initiated at a pore on the boundary or at a triple point. The smooth monotonic increase in specimen length shown in Fig. 3b indicates that such propagation along a grain boundary occurs by stable rather than a dynamic mode.

It should be noted that the presence of cracks in the specimen interior causes a lowering of the effective moment of inertia of the cross-section. For this reason, the strength values for the annealed

specimens shown in Fig. 4 are understated. A detailed quantitative analysis of this effect is beyond the scope of this study. It may be noted that, in principle, relaxation of the compressive stresses in the surface region of the specimen could occur by the extrusion of the viscous glassy grain boundary phase, as observed by Clarke [25] during compressive deformation of glass–crystal composites. Scanning electron microscopy of the surface of the present tempered and annealed specimens failed to give evidence of this effect.

### 3.2. 614 alumina

Fig. 8 shows the thermal expansion behaviour of a tempered specimen of the 614 alumina. This specimen also exhibits an irreversible increase in length over about the same temperature range as the Al-300. Again, this increase in length must be attributed to the formation of cavities or cracks

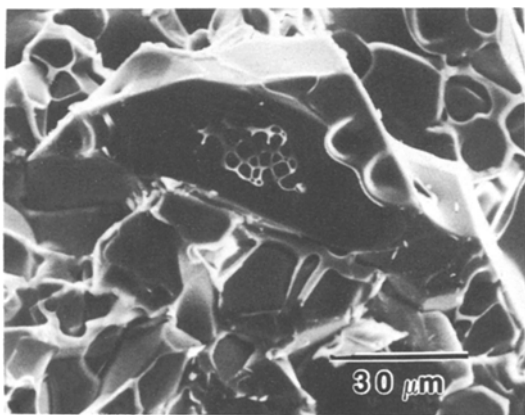


**Figure 6** SEM fractograph showing evidence of viscous deformation of glassy phase during high-temperature anneal.

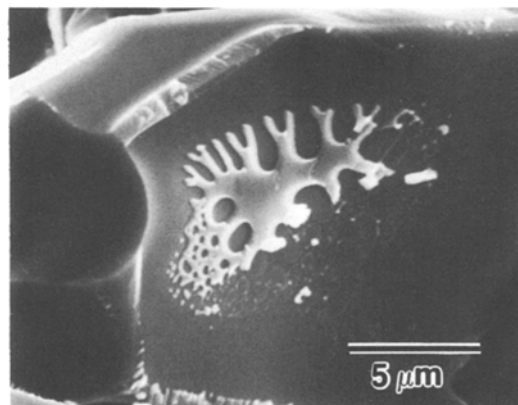


**Figure 7** SEM fractograph showing pattern indicative of crack growth along viscous glassy grain boundary phase.

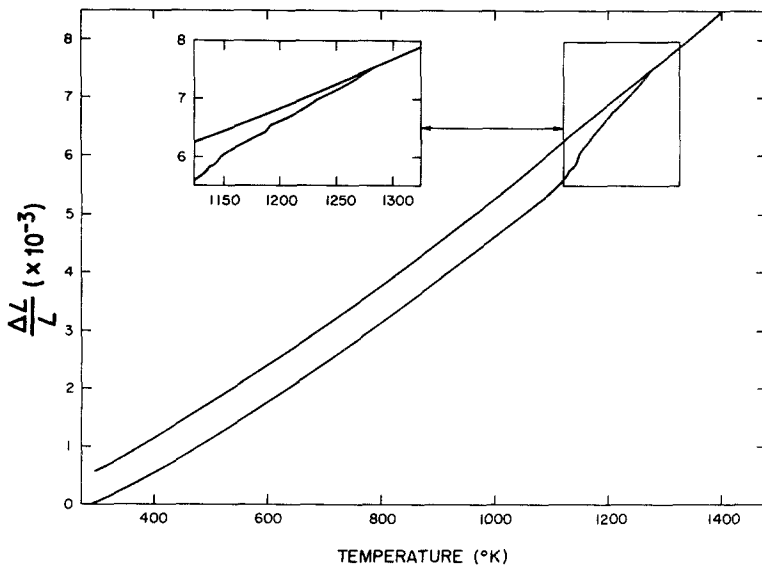


Figure 8 Thermal expansion of tempered 614 alumina.

during heating. However, in contrast to the smooth monotonic increase in length observed for the Al-300, this increase for the 614 alumina appears to be irregular. This suggests that the internal cracking in the 614 alumina involved dynamic (unstable) crack propagation, corresponding to pop-in. The irregular increase in length over a range of temperature suggests that a number of different cracks were involved, each popping-in at a different temperature.

Fig. 9 shows the tensile strength of the tempered rods at room temperature, following the 25 min anneal over a range of temperature. Note that the anneal has decreased the load-bearing ability of

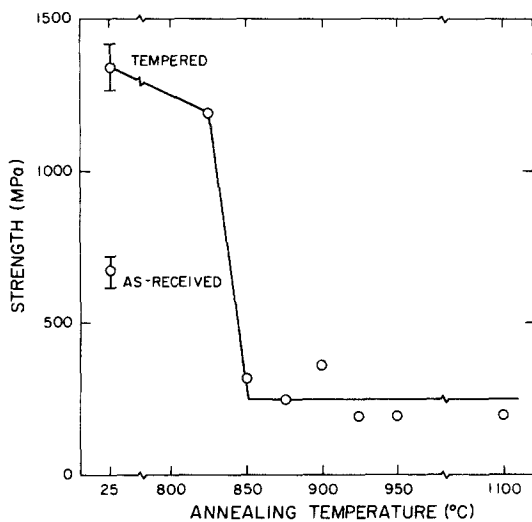


Figure 9 Tensile strength of 614 alumina measured in bending at room temperature following tempering and a 25 min anneal, as a function of annealing temperature.

the tempered rods to a value below that of the as-received specimens. This strength decrease also occurred in a rather precipitous manner over a narrow temperature range, analogous to the strength loss behaviour due to unstable, dynamic crack propagation in brittle ceramics subjected to thermal stresses of high magnitude [26]. Thus, at least two indirect pieces of evidence suggest that the crack formation in the tempered 614 alumina involved unstable crack propagation.

Fig. 10 shows an SEM fractograph of the total face of the specimen broken at room temperature following tempering and a 25 min anneal. This fracture surface indicates the existence of an inner ring concentric with the radial specimen surface. SEM-fractography at higher magnification

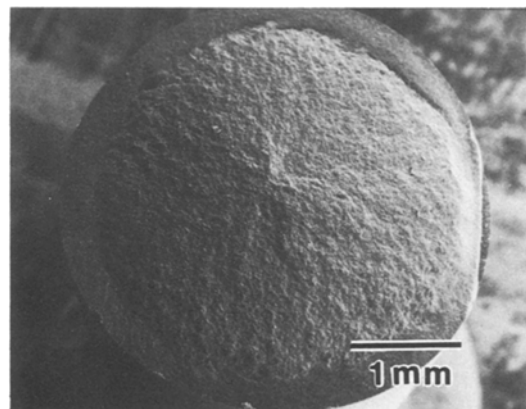


Figure 10 SEM fractograph of specimen of 614 alumina broken at room temperature following tempering and a 24 min anneal at 900°C, showing intergranular crack propagation into compressive stress field.

revealed that the inner ring primarily showed intergranular crack propagation typical of elevated temperatures. The outer ring showed transgranular fracture typical of failure at room temperatures. This suggests that the inner ring represents the extent of crack propagation during the anneal. The outer ring represents the remaining ligament which was fractured at room temperature.

Fig. 11 shows the size of the inner ring relative to the specimen size, as a function of annealing temperature. These data indicate that the size of the inner ring tends to increase with increasing annealing temperature. This effect may be attributed to two phenomenon. Firstly, a decrease in the critical stress intensity factor with temperature would cause the crack on pop-in to propagate further before arrest. Secondly, the higher temperatures of the anneal would permit a greater extent of subcritical crack growth by a thermally activated process during the anneal, following crack pop-in at a lower temperature. This latter explanation is thought to be the more probable of the two.

Attempts to calculate the failure stress from the data shown in Fig. 11 by treating the tempered and annealed rod as a hollow cylinder, gave unsatisfactory agreement with the strength values of the as-received materials. This indicates that the presence of the central crack has an effect on the stress distribution at the surface of the rod. No theoretical solution for this effect appears to be available for a further quantitative analysis of this effect. For this reason, although the data in

Fig. 12 are presented in terms of the failure stress of a solid rod, their relative magnitude should be regarded as indicative of the relative load required to cause specimen failure in three-point bending.

### 3.3. 838 alumina

Fig. 12 shows the thermal expansion behaviour of a tempered specimen of the 838 alumina. A discontinuous change in length occurs at a single value of temperature. For all specimens tested, such an instantaneous change occurred at temperatures ranging from 600 to 900°C. When such a change in length occurred, the specimens frequently broke into two separate pieces, indicative of crack pop-in involving a highly unstable mode of crack propagation.

Fig. 13 shows the strength of the tempered 838 alumina specimens following a 25 minute anneal over a range of temperature, for two values of the initial temperature used in the tempering process. Strength loss due to the crack pop-in is extensive with those specimens which showed complete fracture, exhibiting no strength whatever.

Fig. 14 shows the time period until crack pop-in for four values of annealing temperature. The data points at the zero value of time indicate spontaneous fracture during heating to the annealing temperature. The arrow at 24 h indicates the number of specimens tested which did not fail within the 24 h period. At 800°C, the times-to-spontaneous failure are distributed relatively uniformly over the 24 h period. Such fracture

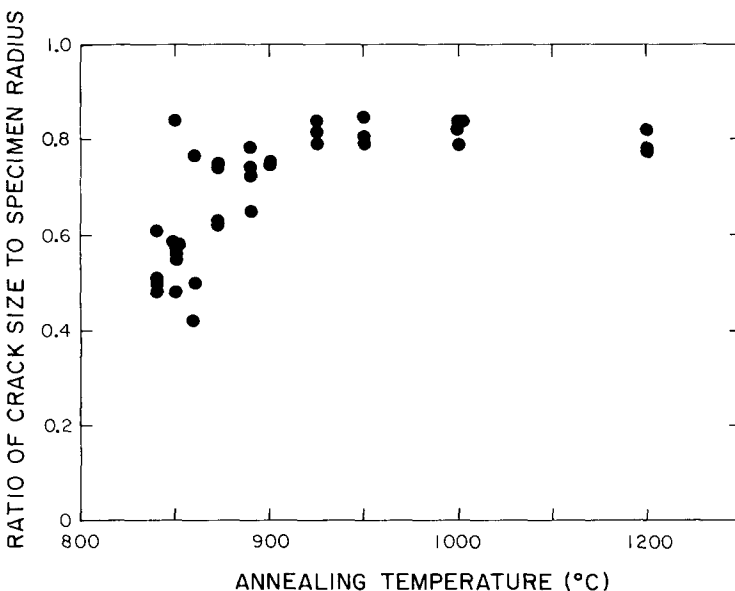


Figure 11 Relative radius of internal cracks in 614 alumina created during 25 min anneal, as a function of annealing temperature.



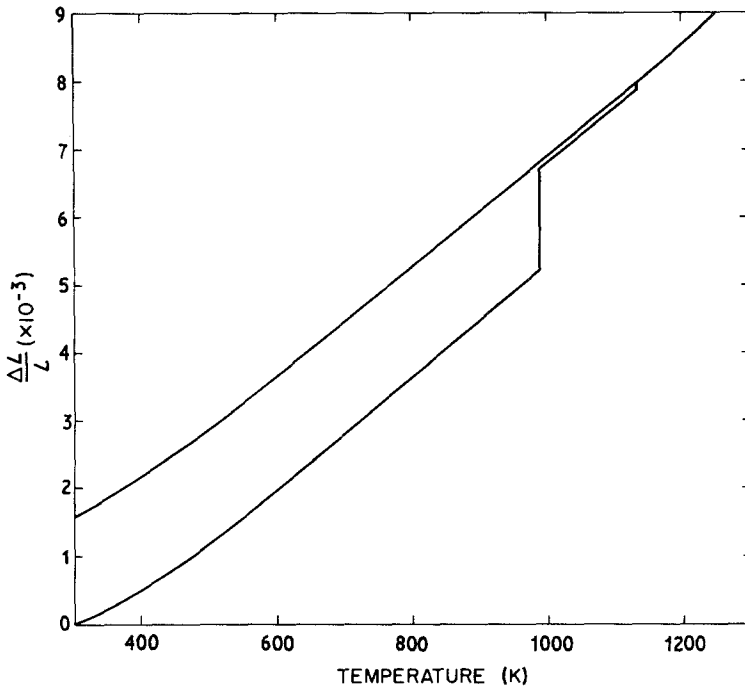


Figure 12 Thermal expansion of tempered 838 alumina.

occurred at temperatures as low as 600°C and as high as 900°C. It is suggested that these data represent evidence of a residual stress induced spontaneous fatigue by subcritical crack growth.

Fig. 15 shows a macro-SEM fractograph of a totally separated specimen. Failure appears to occur by a cup-and-cone type of fracture, possibly related to the nature of the distribution of the

residual stress. Fig. 16 is an SEM-fractograph of what is thought to be the origin of spontaneous fracture. It appears that such failure was initiated at a processing defect. Crack propagation occurred in an intergranular manner expected for high temperature fracture. No evidence was found for the presence of a glassy grain boundary phase.

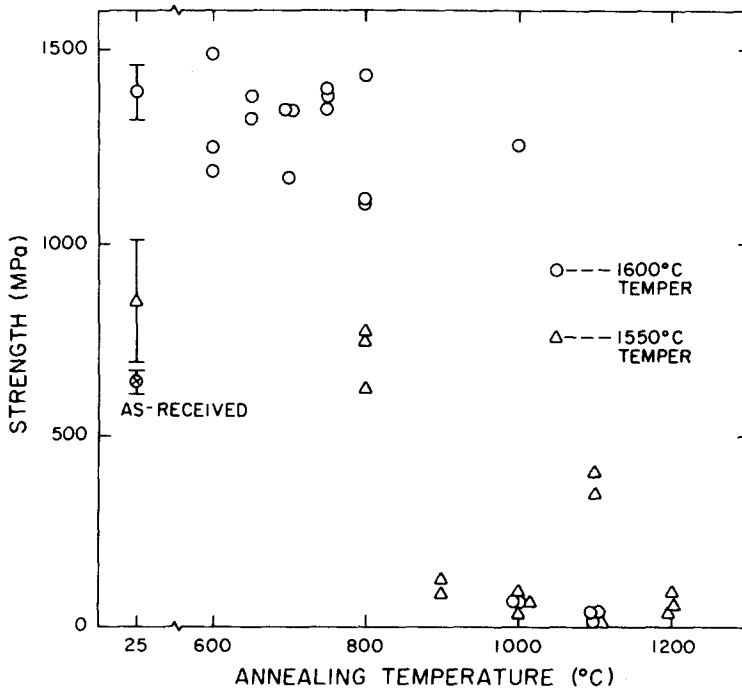


Figure 13 Tensile strength of 838 alumina measured in bending at room temperature following tempering from 1550 and 1600°C and a 25 min anneal, as a function of annealing temperature.

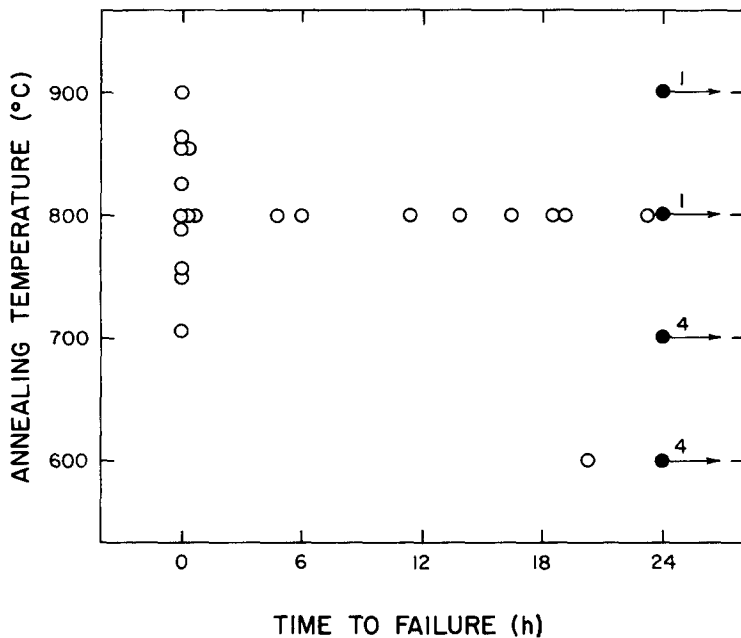


Figure 14 Time-to-spontaneous fracture of tempered 838 alumina for four values of annealing temperature (numbers on arrows indicate the number of specimens which did not fail within 24 h period).

#### 4. Discussion

The residual stress induced cracking reported above, has a number of practical implications. In general, such crack formation is not desirable especially in those materials intended for high load-bearing purposes. Such loss in load-bearing ability will depend on the size, orientation and location of the cracks as well as the distribution of stress during service. In this respect it should be noted that, if a pure tensile strength test had been used in the present study, the resulting relative strength loss would be expected to have been even greater than the reported values obtained in bending.

At least two different mechanisms of crack

growth appear to be operative in the three alumina materials investigated. In this respect, the Al-300 and the 838 alumina must be regarded as the ends of the spectrum. In the Al-300, the glassy grain boundary phase appears to play the primary, if not only, role in the formation of cracks along grain boundaries. Such cracks could originate from bubbles nucleated in the glassy phase by the tensile stresses. More likely, crack growth is initiated at pores on the grain boundaries or triple points, perhaps by the mechanism described by Evans [27]. A quantitative analysis of this effect for purposes of comparison between theory and experiment would require detailed microstructural information on the distribution

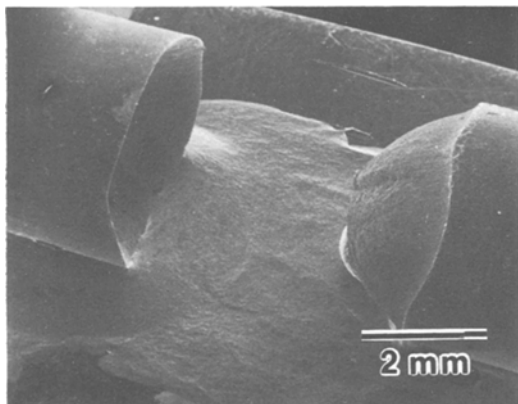


Figure 15 SEM fractograph of spontaneously fractured tempered specimen of 838 alumina annealed at 800°C.

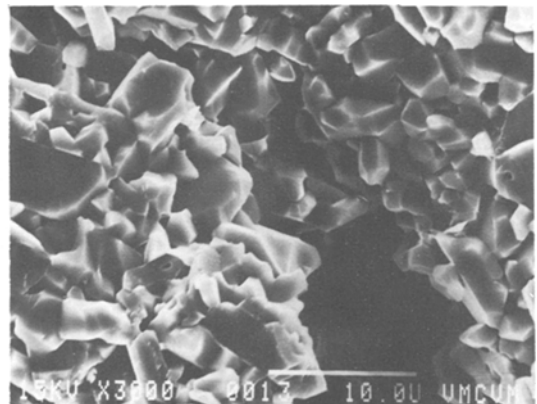


Figure 16 Fracture origin of spontaneously fractured tempered 838 alumina specimen of Fig. 15.

and thickness of the glassy phase and its viscosity, as well as information on the size and geometry of the pore phase. Such an analysis also would be complicated by the strong dependence of the critical stress intensity factor of alumina with a glassy phase on temperature as well as loading conditions [28].

In contrast, in the 838 alumina which doesn't appear to contain a glassy grain boundary phase, subcritical crack growth most likely occurs by a diffusional process such as described by Chuang and Rice [29]. Subcritical crack growth in a high-purity polycrystalline aluminium oxide was observed by Evans and co-workers [30] at temperatures as low as 600° C. Regardless of the details of the mechanisms involved, such crack growth would also be expected to occur in the 838 materials. Indirect evidence for the existence of such crack growth is given by the data for the time-to-spontaneous failure shown in Fig. 14.

In the Al-300 alumina, cracking can occur potentially at every grain boundary oriented perpendicularly to the tensile residual stress. For this reason, the crack formation in the Al-300 alumina is expected to be rather homogeneous. This is supported by the observation that for all specimens tested, the thermal expansion showed the irreversible change in length over the same temperature range. In contrast, crack formation in the 838 alumina appears to be initiated at processing defects. The incidence of fracture then, will depend very strongly on density and size distribution of such defects. For a very low density of defects coupled with large variation in their dimension, fracture due to the residual stresses is expected to show considerable scatter, as evidenced by the large range of temperature over which such fracture was observed.

Crack propagation in the 838 alumina was far more extensive than in the Al-300. For an explanation of this effect, it should be noted that fracture under the influence of residual stresses (in the absence of external forces) is qualitatively identical to crack propagation under the influence of thermal stresses under the same conditions. A theoretical analysis [26] of this latter phenomenon showed the mode and extent of crack propagation to be a function of the number (i.e. density) of cracks which participate in the fracture process. For a high density of cracks, propagation occurs in a stable mode, followed by crack arrest. For a low density of cracks, however, crack propagation

occurs in an unstable manner. This involves extensive crack propagation as the result of the "overshoot" of the crack beyond its dimension for stable crack arrest. Qualitatively identical fracture behaviour should occur under the influence of residual stresses. The Al-300 with its more homogeneous deformation involving high crack density is expected to show far less extensive crack propagation than the 838 alumina in which feature was initiated from just a single or only a few defects.

All three alumina materials of this study were dense and inert to the ambient atmosphere. For this reason, the crack growth due to the tensile residual stresses in the interior of the specimen could occur only at levels of temperature sufficiently high to require thermally activated diffusional or flow processes, rather than by stress corrosion. If, however, the residual stresses were distributed such that the tensile stresses of high magnitude existed at the surface, crack growth by stress-corrosion should be entirely feasible. Rates of crack growth by this latter mechanism at room temperature can exhibit the same rates as diffusional processes at high temperatures [31]. For this reason, spontaneous fracture in residually stressed materials can be encountered at room temperature as the result of stress-corrosion effects. This latter mechanism is offered as an explanation for the spontaneous fracture of residually stressed brittle materials at room temperature, referred to in Section 1.

The measurements of the residual stress fatigue of the 838 alumina for practical reasons covered a 24 h period. No reason exists why the time-to-failure could not extend over longer periods. This will depend on the magnitude of the residual stress, the size and geometry of the precursor flaws as well as the specific mechanism of crack growth and the existence of a fatigue limit. In principle, estimates of times-to-failure can be made on fracture-mechanical principles [31]. However, in the absence of the appropriate detailed information, it must be assumed that residually stressed components or structures have the potential for spontaneous failure.

It is of interest to examine to what extent other creep processes may have contributed to the deformation and residual stress relaxation at the level of temperature of the present experiments. If the decrease in residual stresses in Al-300 over a period of 25 min were due to a linear creep process, the

required effective viscosity would be of the order of  $10^8$  to  $10^9$  MPa sec.

The effective viscosities  $\eta_{\text{NH}}$  and  $\eta_{\text{C}}$  for Nabarro-Herring [17, 18] and Coble [19] creep, respectively, can be written:

$$\eta_{\text{NH}}^{-1} = 20\Omega_{\text{v}}D_{\text{L}}/kTd^2 \quad (1)$$

$$\eta_{\text{C}}^{-1} = 24\Omega_{\text{v}}\delta D_{\text{gb}}/kTd^3 \quad (2)$$

where  $\Omega_{\text{v}}$  is the molecular volume of the diffusing species (Langdon and Mohamed [32]),  $D_{\text{L}}$  and  $D_{\text{gb}}$  are the diffusion coefficients for lattice and grain boundary diffusion, respectively,  $\delta$  is the width of the grain boundary,  $k$  is the Boltzmann constant and  $T$  is the absolute temperature. For these quantities, numerical values can be taken identical to those selected by Langdon and Mohamed [32] with the  $\text{Al}^{3+}$  ion as the rate-controlling atomic species:  $\Omega_{\text{v}} = 4.2 \times 10^{-29} \text{ m}^3$ ,  $D_{\text{L}} = 28 \times 10^{-4} \exp(-478000/8.31T) \text{ m}^2 \text{ sec}^{-1}$ ,  $\delta D_{\text{gb}} = 8.6 \times 10^{-10} \exp(-419000/8.31T) \text{ m}^3 \text{ sec}^{-1}$ .

For a mean grain size of  $4 \mu\text{m}$  for the 838 alumina and a temperature of  $850^\circ\text{C}$  yields  $\eta_{\text{c}}$  and  $\eta_{\text{NH}}$  equal to about  $4 \times 10^{13}$  and  $2 \times 10^{15}$  MPa sec, respectively. Similarly, for a mean grain size of  $25 \mu\text{m}$ ,  $\eta_{\text{NH}} \approx 7 \times 10^{16}$  and  $\eta_{\text{c}} \approx 9.8 \times 10^{15}$  MPa sec. All these values are far greater than the viscosity of  $10^8$  to  $10^9$  MPa sec inferred from the experimental data for the Al-300. Therefore, any effect of diffusional creep on the present observations must be considered negligible and all

observations must be attributed to the formation of cracks. For this reason, the earlier observations [20] of residual stress relaxation in Al-300 cannot be attributed to Coble creep.

The growth of cracks is not expected to occur under conditions of compressive residual stresses. The latter stresses will relax also, because of the coupled nature of the residual stress distribution. For this reason, the relaxation of the tensile stresses by crack formation automatically leads to the decrease of all residual stresses, by the mechanism of "elastic relaxation". For the Al-300 this mechanism is illustrated in Figs. 17a and b which show the original stress distribution in the tempered specimens, and the cracks in the interior of the stress-free specimen following the anneal, respectively.

The elastic relaxation of the compressive stresses must lead to an inevitable change (increase) in dimensions, as observed. The associated strain should be approximately equal to the original elastic strain, depending on the number and size of the cracks which formed, as well as the original residual stress distribution. For components made to very close tolerances, such distortions could present difficulties with proper performance in service.

The experimental results presented in this paper, in particular those for the Al-300 alumina are thought to represent evidence for the existence of creep by crack growth, proposed in an earlier study [21]. It should be noted that creep by this

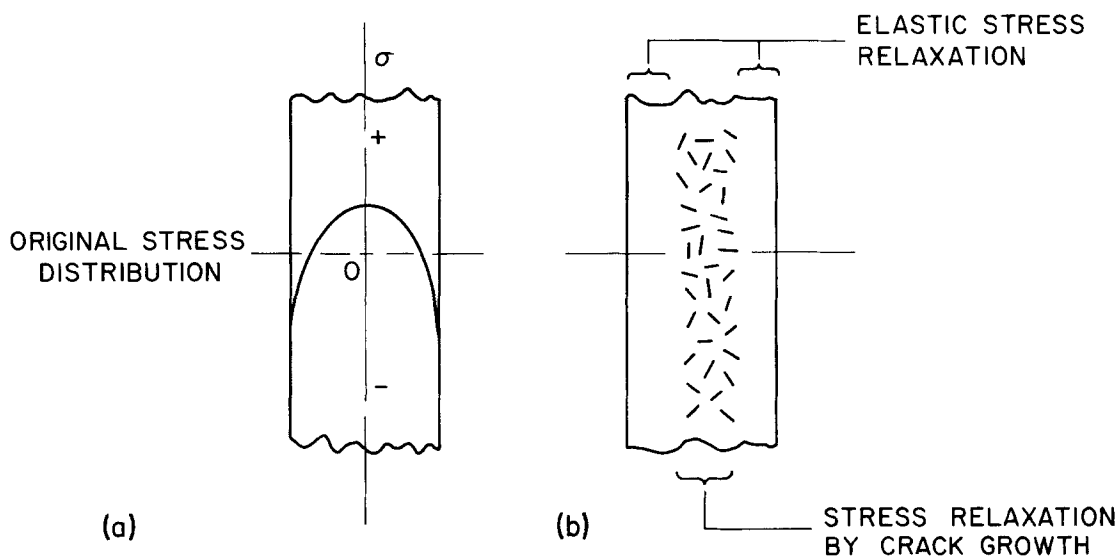


Figure 17 Schematic of residual stress relaxation by crack growth (a) original stress distribution and (b) after annealing treatment.

mechanism may be the dominant, if not only, mechanism of creep regardless of the temperature level, for multi-axial stress distributions which tend to suppress deformation by shear. Because residual stresses tend to be multi-axial, stress relaxation by crack formation may well be encountered even in those materials which exhibit considerable non-linear deformation under a pure or resolved shear stress.

The practice of using a thermal anneal for the purpose of reducing or eliminating residual stresses in brittle ceramics should be examined in the light of the earlier conclusion that at the levels of temperature at which crack propagation occurred, creep by the Nabarro–Herring or Coble mechanisms was negligible. This leads to the inevitable conclusion that if attempts were made to reduce the residual stress in the present samples by diffusional creep, fracture will occur during heating to the appropriate temperatures. When this will occur will depend on the magnitude of the residual stresses and the nature of the defect (pore, etc) at which the fracture originates. In particular, such fracture will depend on the residual stress intensity factor associated with such a defect, relative to the values of stress intensity factor required for crack propagation.

This is illustrated schematically in Fig. 18. The residual stress intensity factor,  $K_{rs}$  is assumed independent of temperature.  $K_0$  represents the minimum value of the stress intensity factor required for subcritical crack growth whereas  $K_{Ic}$  is the critical stress intensity factor for fast fracture. This latter mode of failure will occur at a

temperature  $T_f$  such that  $K_{rs} \geq K_{Ic}$ . Subcritical crack growth and associated residual stress fatigue will occur over the temperature range from  $T_0$  to  $T_f$  such that  $K_0 < K_{rs} < K_{Ic}$ . Whether under the latter condition catastrophic fracture will occur at  $K_{rs} = K_{Ic}$  will depend on the degree of residual stress relaxation due to the crack growth. As discussed earlier, this in turn will depend on the total number (i.e. density) of cracks which take part in the fracture process. Only when  $K_{rs} < K_0$  which occurs at a temperature  $T < T_0$ , no subcritical crack growth will occur. In principle, in this regime of temperature residual stress relaxation can be brought about by diffusional creep, but this can be done only when the temperature  $T_0$  is high enough that the rate of such diffusional creep be sufficiently high that significant stress relaxation can occur within a practical time period. This can be accomplished by keeping the residual stresses as low as possible by careful process control. Furthermore, for any magnitude of residual stress, stress intensity factors can be reduced by minimizing the size of the processing defects. Rates of diffusional Nabarro–Herring or Coble creep can be enhanced by keeping the grain size as small as possible.

Small amounts of other materials (which tend to form a glassy phase) are frequently added to enhance sinterability. However, because of their inherently lower viscosity than for the matrix, grain boundary cracking due to residual stresses is inevitable. For this reason, it is recommended that a glassy grain boundary phase be eliminated. On the other hand, as discussed earlier, crack propa-

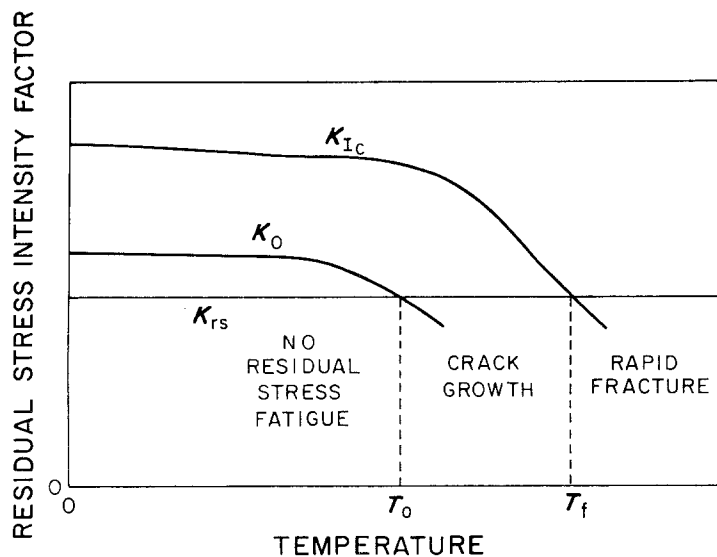


Figure 18 Schematic of relative magnitude of residual stress intensity factor with corresponding values for fast fracture ( $K_{Ic}$ ) and minimum value ( $K_0$ ) required for subcritical crack growth.

gation along a glassy grain boundary phase may be less extensive than in the pure matrix material. For this reason, the presence of a glassy phase could be advantageous. The appropriate choice will depend on the nature of the matrix material, its preferred method of processing and the conditions under which the material is to be employed.

### Acknowledgements

This study was conducted as part of a research project supported by the Army Research Office under Contract No. DAAG 29-79-C-0193.

### References

1. A. G. COCKBAIN, *Proc. Brit. Ceram. Soc.* **25** (1975) 253.
2. A. YU MALININ, V. S. PAPKOV, V. D. CHUMAK and A. P. VIDANOV, *Iz. Akad. Nank SSSR Ser. Fiz.* **37** (1973) 2367.
3. H. P. KIRCHNER, "Strengthening of Ceramics" (Marcel Dekker, Inc., New York, 1979).
4. F. I. BARATTA, *Bull. Amer. Ceram. Soc.* **57** (1978) 806.
5. R. C. POHANKA, R. W. RICE and B. E. WALKER Jr, *J. Amer. Ceram. Soc.* **59** (1976) 71.
6. W. KERSTAN, *Sprechsaal* **113** (1980) 54.
7. R. GARDON and O. S. NARAYANASWAMY, *J. Amer. Ceram. Soc.* **53** (1970) 380.
8. A. R. COOPER and D. A. KROHN, *ibid.* **52** (1969) 665.
9. A. J. DURELLI and W. F. RILEY, "Introduction to Photomechanics" (Prentice-Hall, Englewood Cliffs, NJ, 1965).
10. B. D. CULLITY, "Elements of X-Ray Diffraction", (Addison-Wesley Pub. Co., Reading Massachusetts, 1956).
11. P. J. NORONHA and J. J. WERT, *J. Testing Eval.* **3** (1975) 147.
12. L. GRABNER, *J. Appl. Phys.* **49** (1978) 580.
13. C. P. CHEN, private communication (1980).
14. E. A. FISHER, in "Proceedings of the Workshop, Non-destructive Evaluation of Residual Stress", San Antonio, Texas, August 1975 (NTIAC Publications, San Antonio, Texas, 1975) p. 125.
15. C. C. HSIAO, "Fracture 1977" Vol. 3 (ICF4, Waterloo, Canada, June 1977).
16. D. P. H. HASSELMAN, personal observation.
17. F. R. N. NABARRO, "Report on a Conference on the Strength of Solids", (Physics Society, London 1948) p. 75.
18. C. HERRING, *J. Appl. Phys.* **21** (1950) 437.
19. R. L. COBLE, *ibid.* **34** (1963) 1679.
20. D. A. KROHN, P. A. URICK, D. P. H. HASSELMAN and T. G. LANGDON, *ibid.* **45** (1974) 3729.
21. A. VENKATESWARAN and D. P. H. HASSELMAN, *J. Mater. Sci.* **16** (1981) 1627.
22. J. WEERTMAN, *Trans. ASM* **62** (1969) 502.
23. J. F. LYNCH, C. G. RUDERER and W. H. DUCKWORTH, "Engineering Properties of Selected Ceramic Materials" (American Ceramic Society Inc., 1966).
24. R. J. FIELDS and M. F. ASHBY, *Phil. Mag.* **33** (1976) 33.
25. D. R. CLARKE, in *Materials Science Research, Vol. 14, Surfaces and Interfaces in Ceramic and Ceramic-Metal Systems*, edited by J. A. Pask and A. G. Evans (Plenum Press, New York, 1981) p. 307.
26. D. P. H. HASSELMAN, *J. Amer. Ceram. Soc.* **52** (1969) 600.
27. A. G. EVANS, *Acta Met.* **28** (1980) 1155.
28. K. KROMP and R. F. PABST, *Met. Sci.* **15** (1981) 125.
29. T. J. CHUANG and J. R. RICE, *Acta Met.* **21** (1973) 1625.
30. A. G. EVANS, M. LINZER and L. R. RUSSELL, *Mater. Sci. Eng.* **15** (1974) 253.
31. "Fracture Mechanics of Ceramics" Vols. 1, 2, 3 and 4, edited by R. C. Bradt, F. F. Lange and D. P. H. Hasselman (Plenum Press, New York, 1974, 1978).
32. T. G. LANGDON and F. A. MOHAMED, *J. Mater. Sci.* **13** (1978) 473.

*Received 5 October  
and accepted 13 December 1982*